Mechanical evaluation and design of a multilayered collagenous repair biomaterial

D. Claire Gloeckner,[1] Michael S. Sacks,[1] Kristen L. Billiar,[2] Nathaniel Bachrach[2]

[1]*Tissue Mechanics Laboratory, Department of Bioengineering, 749 Benedum Hall, 3700 O'Hara Street, Pittsburgh, Pennsylvania 15261*
[2]*Organogenesis, Inc., Canton, Massachusetts*

Abstract: One method of fabricating implantable biomaterials is to utilize biologically derived, chemically modified tissues to form constructs that are both biocompatible and remodelable. Rigorous mechanical characterization is a necessary component in material evaluation to ensure that the constructs will withstand *in vivo* loading. In this study we performed an in-depth biaxial mechanical and quantitative structural analysis of GraftPatch (GP), a biomaterial constructed by assembling chemically treated layers of porcine small intestinal submucosa (SIS). The mechanical behavior of GP was compared to both native SIS and to glutaraldehyde-treated bovine pericardium (GLBP) as a reference biomaterial. Under biaxial loading, GP was found to be stiffer than native SIS and mechanically anisotropic, with the preferred fiber direction demonstrating greater stiffness. Quantitative structural analysis using small-angle light scattering indicated a uniform fiber structure similar to GLBP and SIS. To enable test-protocol-independent quantitative comparisons, the biaxial mechanical data were fit to an orthotropic constitutive model, which indicated a similar degree of mechanical anisotropy between the three groups. We also demonstrate how the constitutive model can be used to design layered biocomposite materials that can undergo large deformations. © 2000 John Wiley & Sons, Inc. J Biomed Mater Res, 52, 365–373, 2000.

Key words: submucosa; mechanical behavior; biocomposite; biaxial mechanical testing; fiber kinematics

INTRODUCTION

A popular method in the development of biomaterials for surgical repair and medical devices utilizes chemically modified, biologically derived materials, either in their native form or as chemically treated composites that are both biocompatible and remodelable. One biological source of a collagenous material used in many applications is small intestinal submucosa (SIS). It is a practical, remodelable biomaterial because of its simple membranous configuration, relative uniformity, and abundant availability. It has been used in several forms in vascular applications and repair of the urinary bladder and Achilles' tendon.[1–5] In these studies, SIS was gradually absorbed by the host organism while concurrently being replaced by host tissue.

Although the biological aspects of this material have been well studied,[6–8] its mechanical behavior has not been adequately investigated. Mechanical evaluation is especially important given the fact that SIS is intended for use in high load-bearing applications such as the abdominal wall, large-diameter arteries, and tendon repair. While uniaxial testing has been performed,[9–11] it is insufficient to fully characterize an anisotropic tissue response, because it does not reproduce a physiological loading state and does not allow detection of the interaction between material directions, or "coupling." Inflation burst tests also performed on SIS materials[11] subject the material to complex loading involving both planar and bending stresses, making the analysis difficult to perform and interpret. More recently, Whitson et al. performed a ball burst test wherein a steel ball was pushed into a sheet of an SIS composite material until it ruptured.[5] The *in vivo* two-dimensional stress–strain properties cannot be derived from this test because the stress distribution in the tissue is unknown and is not constant throughout the specimen.

We have previously conducted mechanical and quantitative structural studies on SIS. Structural analysis indicated a single preferred direction, but occasionally two fiber populations oriented at ±30° to the longitudinal axis were detected. Biaxial testing experiments indicated that the material was mechani-

cally anisotropic, with a stiffer preferred fiber direction. We also observed asymmetric cross-coupling between the longitudinal and circumferential material axes, suggesting mechanical interactions at the fiber level.

Potentially, SIS-derived layered composite biomaterials can be designed with a spectrum of mechanical responses for a broad range of applications. The structural consistency of SIS facilitates its use in layers in a composite stacked material, which stands in contrast to the structural variability of other soft tissues, such as bovine pericardium, that exhibit wide variations in structure.[12,13] However, native and chemically treated, biologically derived soft biomaterials undergo large deformations and exhibit complex, anisotropic mechanical responses,[14] so that conventional laminate theory is not applicable in predicting their mechanical response.[15] To mechanically design biocomposites that utilize biologically derived tissues, a large deformation constitutive model is first needed to simulate layer stress–strain properties, then the mechanical behavior of the construct predicted by summing the individual layer responses. Such models can then be utilized alone for simple material geometries, or incorporated into computational methods (e.g., finite-element analysis) for more sophisticated simulations and designs.

In the present study, we performed quantitative structural analyses and multiaxial mechanical testing on a SIS-derived biocomposite material, GraftPatch (GP), a multilayered composite of processed SIS (Organogenesis, Inc., Canton, MA) (Fig. 1). An orthotropic constitutive model was used for both GP and native SIS to facilitate test protocol-independent comparisons. Results were also compared to glutaraldehyde-treated bovine pericardium, a commonly used biologically derived biomaterial. Finally, we demonstrate how the orthotropic constitutive model can be used to design biocomposites with a range of mechanical properties.

MATERIALS AND METHODS

Specimen preparation

The GP material was constructed from SIS prepared from the intestines of swine ($\geq$200 kg) obtained from a closed herd (Parsons Farm, Hadley, MA) as follows. The mesenteric layer was manually removed from the small intestine prior to mechanical stripping of the mucosal and membranous layers. It was mechanically processed on a modified apparatus (Model M34, Ernest Bitterling, Nottingham, UK). The remaining submucosal intestinal collagen layer (ICL) was slit longitudinally between the lymphatic tags and cut into 15-cm lengths that were chemically processed to remove any residual cellular debris. The chemical cleaning of
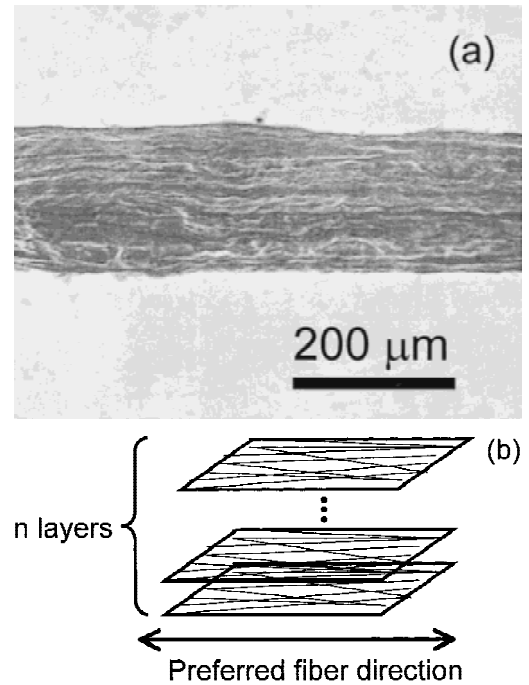

Figure 1. (a) Cross-section of GraftPatch demonstrating its tight, layered structure (original magnification ×100), and (b) the schematic of the six-layered construction of GraftPatch.

the intestinal collagen layer is a proprietary process involving a series of washes in ethylene-diamine tetraacetic acid (EDTA) and NaCl at specific pH ranges.[16] This final material was stored at −80°C until use.

The GP constructs were formed by layering six individual sheets of ICL on top of each other [Fig. 1(b)], with the serosal (abluminal) side of the ICL facing up, and drying them overnight in a laminar flow hood. The layered constructs were chemically crosslinked for 8 h with 100 mmol/L ethyl-3(3-dimethylamino)-propylcarbodiimide (EDC; JBL Scientific, San Luis Obispo, CA) in a 50% acetone solvent. After crosslinking, the constructs were sterilized in 0.1% peracetic acid for 8 h and rinsed three times with deionized water, hermetically sealed in foil bags, and sterilized by gamma irradiation at a dose of 25–35 kGy.

The final composite has a total thickness of ~250 μm and is approximately 95% collagen. Six tissue sections of GP material were sent to our laboratory in individually sealed plastic pouches (Table I), and kept sealed and refrigerated until testing. Prior to testing, tissue sections were soaked in physiological saline at room temperature for 1 h to ensure full rehydration. For the mechanical testing, a 20 mm × 20 mm specimen was cut from a relatively avascular region[17] of the section in a stress-free state, with sides aligned to the circumferential and longitudinal directions. Previous work showed that the longitudinal axis of the intestine, identifiable in a tissue section by the pattern of the vasculature, is the preferred fiber direction.[17] Original thickness was measured with a caliper (0.0254-mm resolution) at six locations on the sample and the average used to compute stress.

The GP material data were compared with two tissue groups, glutaraldehyde-treated bovine pericardium (GLBP) and native SIS. GLBP was chosen because it is a commonly

TABLE I
Biaxial Testing Protocol and Maximum Loading for Each Specimen Group

Run No.	SIS (Stretch Control)		GP (Stress Control) Maximum Stresses (kPa)		GLBP (Stress Control) Maximum Stresses (kPa)	
	PD	XD	PD	XD	PD	XD
1	1.12	1.12	800	800	1000	1000
2	1.12	1.04	800	267	500	1000
3	1.12	1.06	800	400	750	1000
4	1.12	1.12	800	800	1000	1000
5	1.06	1.12	400	800	1000	750
6	1.04	1.12	267	800	1000	500
7	1.12	1.12	800	800	1000	1000

used reference biomaterial, whereas native SIS was used for comparison as an unprocessed native tissue. The GLBP specimens were prepared as previously described.[14] Briefly, fresh bovine pericardium was obtained from a local abattoir, which was defatted by blunt dissection and then fixed in a 0.625% aqueous glutaraldehyde 0.9% solution for 24 h at 4°C. A small-angle light-scattering (SALS)-based tissue sorting procedure was used to select the BP biaxial specimen with a uniform collagen fiber structure. Specimens were cut from the pericardial section with their edges aligned with the preferred and cross-preferred fiber directions. The natural SIS specimens were obtained using methods described in detail in Sacks et al.[17] Both GLBP and SIS specimens were kept refrigerated at 4°C in saline until testing.

Structural evaluation

A detailed description of the SALS device, analysis methods, and its accuracy in tissue structural analysis,[18] as well as its application to SIS,[17] have been presented previously. The essential information obtained from SALS is the angular distribution of scattered light intensity about the laser axis, $I(\Phi)$, which represents the distribution of fiber angles within the light beam envelope at the current tissue location. Because different tissues and chemical treatments will result in different tissue optical properties, it is not possible to compare directly the $I(\Phi)$ intensity distributions. To enable this comparison, we normalized $I(\Phi)$ to a unit area for each tissue tested. Note that, because the intensity distribution was symmetric about 180°, only half of the total 360° was needed to reproduce the complete distribution.[18] This results in the probability density function $R(\Phi)$, representing the angular distribution of fibers, computed using:

$$R(\Phi) = \frac{I(\Phi)}{\sum_{-90°}^{90°} I(\Phi)\Delta\Phi} \qquad (1)$$

Prior to SALS testing, tissue specimens were optically cleared using graded glycerol solutions at room temperature to a final 100% solution. In this study, the fiber preferred direction angle, Φ, was measured in discrete 1° increments with respect to the longitudinal axis of the small intestine

from which the samples were taken [Fig. 2(a)]. All specimens were SALS tested using a 1.27-mm-spaced rectilinear grid with a ~1-mm laser-beam diameter.

Biaxial mechanical testing

In our previous SIS work, stretch control was used because we were interested in examining the native fiber ki-
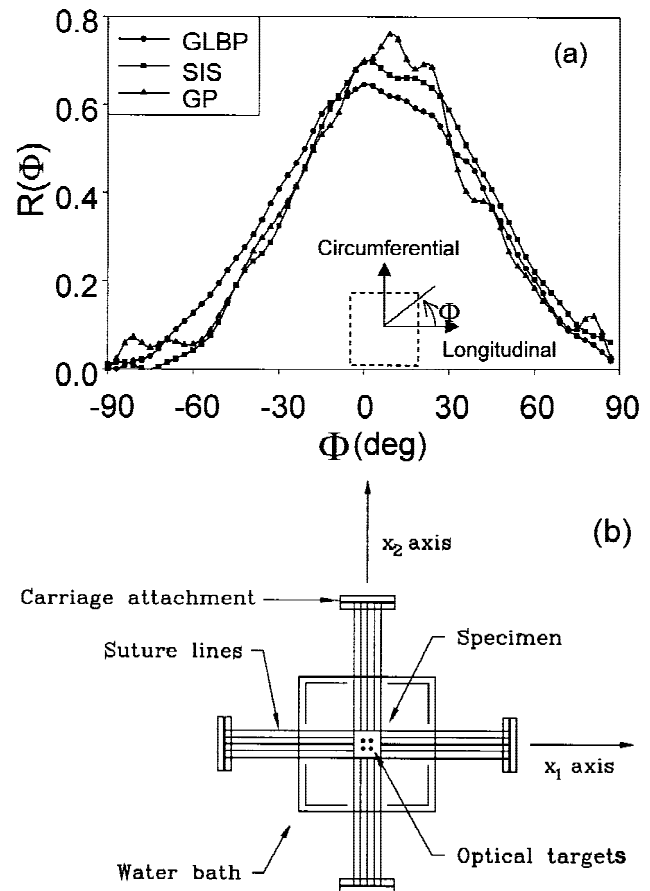

Figure 2. The normalized fiber orientation distribution, $R(\Phi)$, for GLBP, SIS, and GP, demonstrated a similarity in gross fiber structure. For all tissues, the preferred fiber direction is 0°.

nematics under known deformations. However, GP was observed to be very stiff, resulting in small deformations. Because the load signals had substantially higher signal-to-noise ratios, a test protocol based on stress provided better control than one based on stretch. Another consideration was that a stress-based protocol was considered to be more physically representative of actual *in vivo* loading conditions. Thus, for GP and GLBP, we chose stress-based control. For native SIS, all results reported in this study were taken from our previous SIS study, in which stretch control was used.[17]

Biaxial testing procedures have been described in detail elsewhere.[14,17] Briefly, each side of the square test specimen was attached to the motor carriages with a surgical staple at each end of a pair of 000 suture lines [Fig. 2(b)]. Opposite the staples, the two loops encircled small pulleys on each side of a horizontal common axle connected in turn to a vertical pivoting rod, thus allowing near-frictionless rotation in three dimensions. Each pulley ensured that the force on each line end was equal and the pivoting rod ensured that the forces were the same in each pair of suture lines. Load was monitored in the two orthogonal axes by two load cells and the in-plane strain was determined by calculating the centroids of four black markers affixed to the surface of the specimen. The Green's strain (E) along each test axis was calculated from the stretch ratio (λ) using:

$$E = \frac{1}{2}(\lambda^2 - 1)$$

Both the load and deformation in each axis were continuously recorded at 12–15 Hz during testing. All specimens were tested in physiological saline at room temperature.

Each test consisted of 12 contiguous cycles with a period of 20–30 s, with a total of seven runs (Table I). Testing began with equi-biaxial preconditioning to the maximum stress level (Table I). Next, five consecutive tests were performed in which the axial ratios of the stresses were maintained at values of 3:1, 2:1, 1:1, 1:2, and 1:3. These ratios were chosen to determine the mechanical behavior over a wide range of stress states. A final equi-biaxial test was performed to confirm that the mechanical behavior had not changed during the experiment. Total testing time was approximately 90 min for each specimen.

Soft tissues undergo large deformations when the applied loads are small, making reference dimensions difficult to identify. Furthermore, the effects of preconditioning are not well understood. Following our methods used for native SIS,[17] we recorded the positions of the optical markers at three stages during mechanical testing. The first measurement was obtained in the unloaded state, with the specimen free floating in the bath. The second set of marker positions was taken after the sample had been attached to the device and a 0.5-g load applied to both axes. The preconditioned reference state was considered to be the most physiological-like state,[19] and produced the most stable stress–strain response. Thus, the marker positions recorded after the first preconditioning run (run 1, Table I) were used for all subsequent strain computations.

Constitutive modeling

In addition to facilitating our biomaterial design goals, constitutive modeling allows for test-protocol-independent quantitative comparisons between tissue groups. Following our previous study on chemically treated tissues,[14,20,21] we assumed that each specimen could be modeled as a hyperelastic material following the assumption of pseudo-elasticity,[14,22] so that the in-plane second Piola–Kirchhoff stresses (S_{ij}) could be derived from a two-dimensional strain energy function, W, using:

$$S_{ij} = \frac{\partial W}{\partial E_{ij}} \tag{2}$$

For the form of W, we used the following orthotropic strain energy density function:

$$W = b_0\left[\exp\left(\frac{1}{2}b_1 E_{PD}^2\right) + \exp\left(\frac{1}{2}b_2 E_{XD}^2\right)\right. $$
$$\left. + \exp(b_3 E_{PD} E_{XD}) - 3 \right] \tag{3}$$

where b_i are the material constants, and E_{PD} and E_{XD} are the Green's strain in the preferred and cross-preferred directions, respectively. Note that, in this form of the strain energy density, negligible shear strains are assumed, which is justified by the results from our previous study.[17] We used Lagrangian stress (T_{ij}, force/original cross-sectional area), as this stress measure is more physically intuitive, and was used for experimental control. Using $T_{PD} = \lambda_{PD} S_{PD}$, $T_{XD} = \lambda_{XD} S_{XD}$, and Eqs. (2) and (3), the resulting expressions for the stresses are:

$$T_{PD} = \lambda_{PD} b_0\left[b_1 E_{PD}\exp\left(\frac{1}{2}b_1 E_{PD}^2\right)\right.$$
$$\left. + b_3 E_{XD}\exp(b_3 E_{PD} E_{XD}) \right]$$
$$T_{XD} = \lambda_{XD} b_0\left[b_2 E_{XD}\exp\left(\frac{1}{2}b_2 E_{XD}^2\right)\right.$$
$$\left. + b_3 E_{PD}\exp(b_3 E_{PD} E_{XD}) \right] \tag{4}$$

All biaxial protocols were fit simultaneously so that a wide range of stress states was used to determine the material constants, b_i. A Levenberg–Marquardt nonlinear curve-fitting algorithm[23] was used to determine the material constants.

Biomaterial design of SIS-derived composites

To simulate layered biomaterials that utilize similar fabrication procedures as GP, but also vary individual layer orientations, we first estimated the mechanical response of a single layer from the GP biaxial mechanical data. Because GP is constructed from six layers of processed SIS with the layers oriented in the same direction [Fig. 1(b)], response of a single layer was computed as one sixth of the intact material using Eq. (4); that is:

$$T_{PD}^{layer} = T_{PD}/6, \ T_{XD}^{layer} = T_{XD}/6$$

Next, we used standard tensor transformation formulas[15] to compute the biaxial mechanical stresses of each layer at any orientation with respect to the PD axis. The net stress–strain response of the biocomposite was then determined by summing the contributions of the individual layers. For simplicity, any interlayer mechanical interactions were ignored and only a simple biaxial strain state, where the shear strains were zero, was simulated. For the biocomposite simulations, we utilized layer orientations of 0:90, −30:30, −20:20, and 0:0 to explore the full potential range of mechanical anisotropy of the final biomaterial. Furthermore, a synthetic strain-based protocol was used to simplify simulation computations, because a stress-based protocol would require numerical inversion of Eq. (4).

RESULTS

Structural analysis

Similar to our previous results with natural SIS,[17] the GP SALS data demonstrated a high signal:noise ratio with a single preferred fiber direction and similar overall shape [Fig. 2(a)]. Unlike native SIS, no regions of dual populations were found. The shape of the $R(\Phi)$ distribution was also very similar to GLBP. The similar structure of these tissues suggests that the mechanical behavior would also be qualitatively similar between specimens.

Biaxial stress–strain behavior

Good biaxial mechanical testing control was observed for all specimens, with better stress control for the GP and GLBP specimens than for the stretch control of the SIS group because of the higher resolution in the load transducers (~0.1 g) than in the video-marker tracking (~0.3% strain). The increased processing of the GP and GLBP specimens resulted in a more stable response throughout testing compared with natural SIS. All groups were mechanically anisotropic, with the preferred fiber direction axis exhibiting the greatest stiffness. The GP specimens were much stiffer than either SIS or GLBP, extending only to a Green's strain of ~0.04 under ~800-kPa peak stress (Fig. 3).

An interesting observation in this study was the presence of different shapes of the non–equi-biaxial stress–strain curves for the preferred direction and cross-preferred direction. In particular, there was a tendency for the preferred direction strain to become negative when the ratio of the axial stresses was 1:3 [Fig. 4(a)]. This indicated strong asymmetric mechani-
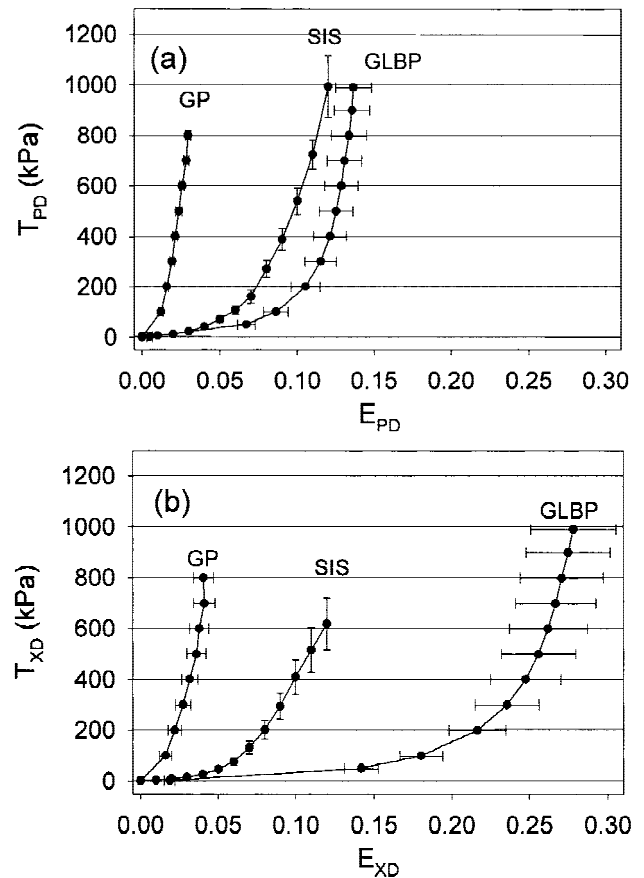

Figure 3. Mean and standard error (SEM) stress–strain behavior of SIS ($n = 6$), GP ($n = 6$), and GLBP ($n = 13$) in the (a) preferred and (b) cross-preferred directions.

cal coupling, where the stress in one axis affects the strain in a perpendicular axis more strongly than in the reverse case. This response did not occur for the corresponding test (3:1) along the cross-preferred axis [Fig. 4(b)]. These results suggest the presence of asymmetric mechanical cross-coupling for SIS-derived materials, most likely the result of the angular arrangement of collagen fibers as seen in natural SIS.[17]

Constitutive model

The biaxial behavior of all individual specimens was modeled very well by Eq. (4), with a mean r^2 of 0.95 or higher (Table II). This included the negative strains in the preferred direction when the preferred direction stress was less than the cross-preferred stress in the 1:3 run [Fig. 4(a)]. Furthermore, the consistency in tissue structure and mechanical behavior manifested itself as low variability in material constants (Table II). The similarity in $R(\Phi)$ for all tissues suggested that their degree of mechanical anisotropy should be similar [Fig. 2(a)]. Because the stress–strain
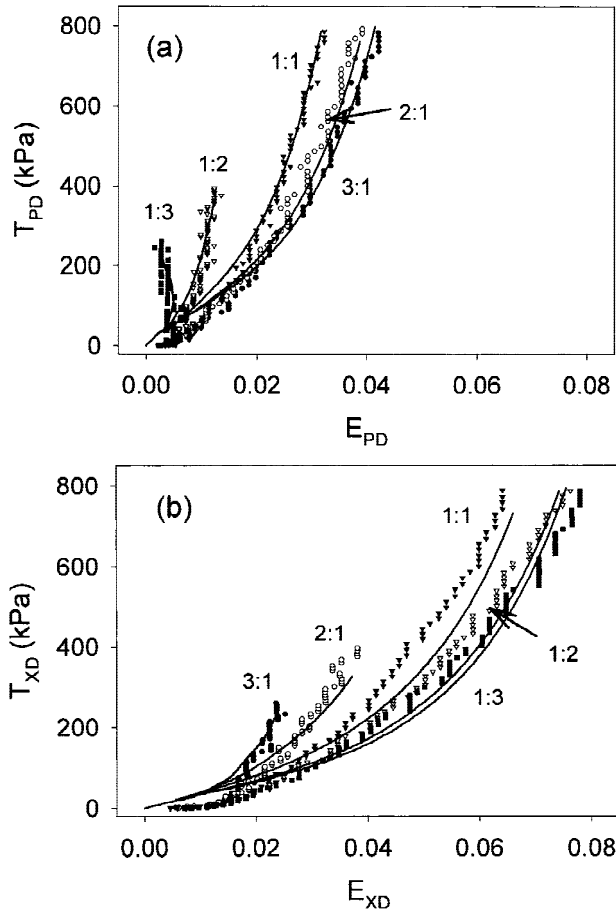
Figure 4. Stress–strain behavior of the GP for all biaxial testing protocols (symbols) and the corresponding fit of Eq. (4) (lines) for the (a) preferred and (b) cross-preferred fiber directions. Eq. (4) fit all the data well, including the negative strain for the 1:3 run in preferred fiber direction in (a).

curves were nonlinear, direct computation and comparison of elastic moduli were not possible. Instead, we used the ratio b_1/b_2 as an index of the anisotropy of the material. Although the GP and SIS mean mechanical anisotropy indices were somewhat smaller than GLBP, overall all specimens exhibited a similar, generally moderate degree of mechanical anisotropy, with values ranging between 1.63 and 3.12 (Table II).

To express varying degrees of mechanical anisotropy, we utilized the ratio of the predicted peak axial stresses, T_{11}/T_{22}, under an equi-biaxial strain state. Results for the layer simulations indicated moderate changes in peak axial stresses over the range of layer orientations [Fig. 5(b)]. Specifically, for GP layers, the T_{11}/T_{22} ratio could be varied from 1:0 (isotropic) to 1.4 for layer orientations ranging from parallel (0:0) to perpendicular (0:90), respectively. Because GP layers are not highly anisotropic, the net mechanical anisotropy at the various orientations was not dramatic. However, the changes were significant and may be important when subtle control of mechanical anisotropy is required.

DISCUSSION

In this study, we examined the structure-strength response of a SIS-derived biocomposite. Similar to our findings for native SIS, GP is mechanically anisotropic with the preferred fiber direction exhibiting the greatest stiffness. The structural consistency of GP specimens resulted in both reasonably consistent mechanical responses and values for the material constants. The fact that GP was much stiffer than GLBP (Fig. 3) may be the result of its more uniform structure and differences in chemical treatment. This finding is supported by the lower b_1/b_2 ratio for GP compared with SIS (Table II), which may be a result of binding between layers not present in natural SIS. In any case, our results suggest that the GP may be more suitable in applications where the deformation must be small while the applied loads are high. In addition, the mechanical anisotropy of GLBP is twice that of GP, indicating that GP may be a better repair material for applications that require more isotropic materials.

The mechanical tests in this study were run at an ambient temperature of ~21°C, and not at 37°C. Studies by Kang et al.[24] and Rigby et al.[25] suggest that temperature differences in this range do not appreciably affect the quasi-static mechanical properties of collagenous tissues. Thus, although we did not test at 37°C, and also that we concentrated on quasi-static properties, it is unlikely that the 15°C difference in temperature would produce measurable differences in mechanical properties.

Soft tissues are also well known to be strain-rate insensitive over several orders of magnitude.[19] In the current study, the deformation rate was slow, on the order of ~1%/s. Thus, the responses at higher or lower physiological strain rates would likely be quite similar to those reported here. Finally, we directly compared the responses of SIS and GP, which were mechanically preconditioned and tested using different loading protocols. The same tissues preconditioned to different protocols will generally yield different, qualitatively similar but quantitatively different, mechanical responses. Even with these study limitations, comparison of these two tissues was of sufficient importance to be included.

Biomaterial design of SIS-derived composites

In the present study, we performed mechanical property simulations that assumed negligible interlayer interactions and utilized only simple loading states that excluded shear strains. This allowed us to perform simulations that demonstrated some of the possibilities of biomaterial design without the need for

TABLE II
Material Constants for Eq. (4) to Individual and Group Specimen Data Sets

Group	b_0 (kPa)	b_1	b_2	b_3	r^2	b_1/b_2
SIS	4.29 ± 0.78	202.47 ± 6.29	104.32 ± 18.88	135.93 ± 8.20	0.96 ± 0.01	2.51 ± 0.71
GP	6.88 ± 1.09	1245.59 ± 110.05	883.21 ± 154.23	648.86 ± 95.75	0.95 ± 0.01	1.63 ± 0.30
GLBP	0.97 ± 0.18	395.77 ± 58.62	126.85 ± 32.75	122.13 ± 26.54	0.96 ± 0.006	3.12 ± 0.48

more complex approaches. This limited our simulations to layer orientations that are symmetric.

However, recent improvements to our biaxial testing device allow for the unique capacity to induce significant amounts of in-plane shear strains.[21] With this information, the prediction of the biocomposite response to any stress state or any combination of layers at any orientation can be determined. Mechanical studies that include shear strains would also facilitate the study of interlayer bonding, because, under this deformation, shearing between layers of different orientations could occur. More advanced approaches include incorporation of Eq. (4) into finite-element software for simulations of not only layer orientation, but more complex stress states, such as those that may be encountered *in vivo*.
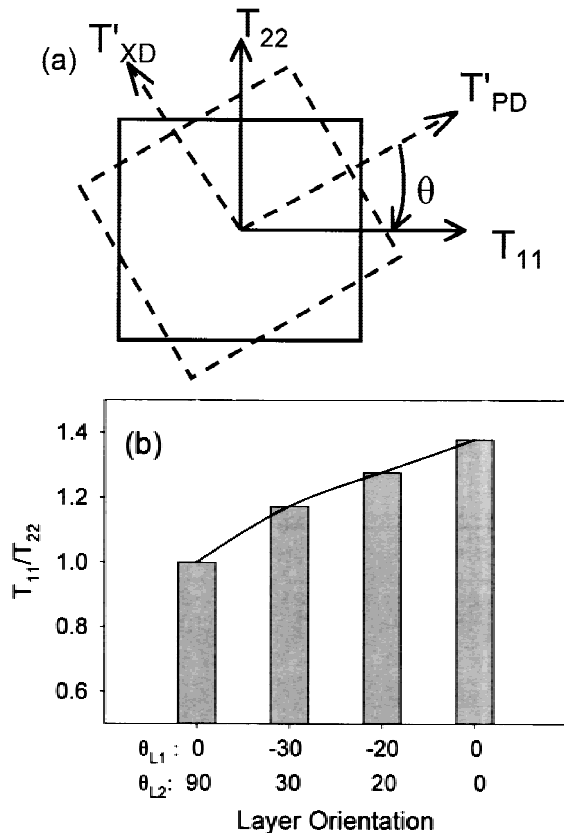

Figure 5. (a) Schematic of the rotation of the individual layers with respect to the preferred and cross-preferred directions of the fibers, with T_{11} and T_{22} representing the net Lagrangian stresses. (b) Prediction of the degree of anisotropy in an engineered construct made of two layers of processed SIS at different orientations.

Phenomenological versus structural constitutive models

Eq. (4) provides a good predictive model of the tissue mechanical response under a wide range of loading conditions. However, this phenomenological approach gives no insight into the contribution of the different components of the tissue to the overall stress–strain response. Alternately, structurally based constitutive models attempt to exploit the tissue composition and structure to avoid ambiguities in material characterization, and offer insight into the function, structure, and mechanics of tissue components.[26–28] This approach is particularly attractive for examining the mechanical behavior of chemically treated tissues. For example, we used a structural approach for chemically treated bovine pericardium to demonstrate the relative contributions from chemically modified collagen fibers and matrix.[29,30]

Critical to the formulation of any structurally guided model is knowledge of how the fibers deform in response to global tissue strains. Prior models assume an affine deformation, where the fibers are assumed to rotate and stretch in the same way as the bulk tissue. When a tissue is chemically treated, and especially when it is bonded together to form biocomposites, fiber mobility behavior may change. Although we originally preferred to utilize a structural approach, the native SIS collagen-fiber mobility under biaxial stretch needed to be established first, which was beyond the primary scope of our study.

To examine the feasibility of developing a structural model for native SIS, however, we utilized the same device to determine how the collagen fibers rotate under biaxial strains. Three native SIS samples were prepared as per our established methods, and mounted onto our novel combined SALS/biaxial stretch apparatus.[31] Each specimen was first SALS scanned before deformation and at three stretch levels of ($\lambda_{PD}:\lambda_{XD}$): 1.12:1.12, 1.30:1, and 1:1.30. The fiber distribution after an equi-biaxial stretch of 1.12:1.12 (see Fig. 9 in ref. 17) and 1.30:1 were both very similar to the corresponding fiber distribution computed from affine deformation theory [Fig 6(a)].[32] However, in the sample stretched to 1:1.30, the single-fiber distribution split into a dual-fiber distribution with peaks at ~50° from the center of the single distribution [Fig. 6(b)].

The basis for this unusual behavior can be explained as follows. It has been shown that SIS consists of two
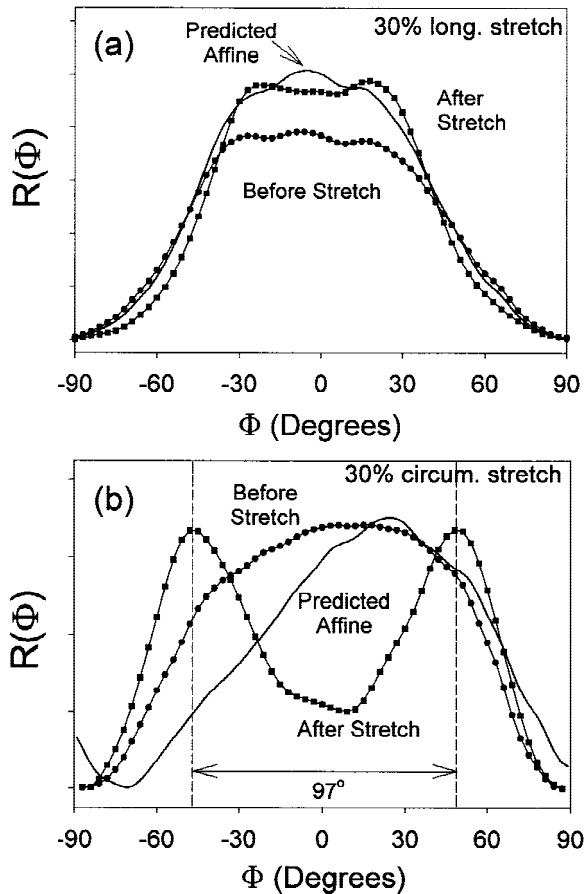
Figure 6. The angular distribution of collagen fibers of a SIS specimen determined before (circles) and after (squares) 30% stretch in the (a) preferred and (b) cross-preferred fiber directions. The separation of the single-fiber population into dual populations after stretch was poorly predicted by the affine deformation model (lines).

fiber populations oriented at ±30° from the preferred fiber direction.[17,33,34] We have also demonstrated that the two fiber populations usually overlap sufficiently, so that only a single-fiber population is detectable.[17] The current results indicate that, under large circumferential strains, the two populations rotate with respect to each other and become distinguishable. These results suggest extreme nonaffine fiber kinematics for native SIS. Clearly, a more in-depth understanding of the fiber kinematics of this tissue is required before a structural model can be developed for native, and ultimately chemically modified, SIS materials.

In summary, the present study investigated the structure–mechanical behavior relationship of a biomaterial fabricated from processed SIS using biaxial testing techniques. The material demonstrated mechanical anisotropy and had a stiffer direction corresponding to the preferred fiber direction. A phenomenological constitutive model for the mechanical behavior was developed, and its potential use in the design of layered composite biomaterials was demon-

strated. Advantages of structural modeling were also discussed, particularly with regard to understanding the contributions of the crosslinks created by processing methods. However, preliminary fiber kinematics studies on native SIS demonstrated that current structure-based models are not adequate for describing the fiber kinematic behavior of native SIS.

References

1. Badylak S, Tullius R, Kokini K, Shelbourne O, Klootwyk T, Voytik SL, Kraine MR, Simmons C. The use of xenogeneic small intestinal submucosa as a biomaterial for Achilles' tendon repair in a dog model. J Biomed Mater Res 1995;29:977–985.
2. Badylak SF, Lantz, GC, Coffey A, Geddes LA. Small intestinal submucosa as a large diameter vascular graft in the dog. J Surg Res 1989;47:74–80.
3. Clarke K, Lantz G, Salisbury K, Badylak S, Hiles M, Voytik S. Intestine submucosa and polypropylene mesh for abdominal wall repair in dogs. J Surg Res 1996;60:107–114.
4. Lantz GC, Badylak SF, Coffey AC, Geddes LA, Blevins WE. Small intestinal submucosa as a small-diameter arterial graft in the dog. J Invest Surg 1990;3:217–227.
5. Whitson B, Cheng B, Kokini K, Badylak S, Patel U, Morff R, O'Keefe C. Multilaminate resorbable biomedical device under biaxial loading. J Appl Biomed Mater Res 1998;43:277–281.
6. Badylak SF, Coffey AC, Lantz DVM, Tacker WA, Geddes LA. Comparison of the resistance to infection of intestinal submucosa arterial autografts versus polytetrafluoroethylene arterial prostheses in a dog model. J Vasc Surg 1994;19:465–472.
7. McPherson T, Badylak S. Characterization of fibronectin derived from porcine small intestinal submucosa. Tissue Eng 1998;4:75–83.
8. Sandusky GE, Lantz GC, Badyluk SF. Healing comparison of small intestine submucosa and ePTFE grafts in the canine carotid artery. J Surg Res 1995;38:415–420.
9. Badylak SF. Small intestinal submucosa (SIS): a biomaterial conducive to smart tissue remodeling. In: Bell E, editor. Tissue Engineering: current perspectives. Boston: Birkhauser; 1993. p 179–189.
10. Herbert ST, Badylak SF, Geddes LA, Hillberry B, Lantz GC, Kokini K. Elastic modulus of prepared canine jejunum, a new vascular graft material. Ann Biomed Eng 1993;21:727–733.
11. Hiles MC, Badylak SF, Lantz GC, Kokani K, Geddes LA, Morff RJ. Mechanical properties of xenogeneic small-intestinal submucosa when used as an aortic graft in the dog. J Biomed Mater Res 1995;29:883–891.
12. Hiester ED, Sacks MS. Optimal bovine pericardial tissue selection sites—Part I: Fiber architecture and tissue thickness measurements. J Biomed Mater Res 1998;39:207–214.
13. Hiester ED, Sacks MS. Optimal bovine pericardial tissue selection sites—Part II: Cartographic analysis. J Biomed Mater Res 1998;39:215–221.
14. Sacks MS, Chuong CJ. Orthotropic mechanical properties of chemically treated bovine pericardium. Ann Biomed Eng 1998;26:892–902.
15. Christensen RM. Mechanics of composite materials. New York: Wiley; 1979. p 348.
16. Abraham GAR, Carr M Jr, Kemp P, Baker L. Chemical cleaning of biological material, U.S. patent application PCT/US98/09432. Canton, MA: Organogenesis Inc.; 1998.

17. Sacks MS, Gloeckner DC. Quantification of the fiber architecture and biaxial mechanical behavior of porcine intestinal submucosa. J Biomed Mater Res 1999;46:1–10.

18. Sacks MS, Smith DB, Hiester ED. A SALS device for planar connective tissue microstructural analysis. Ann Biomed Eng 1997;25:678–689.

19. Fung YC. Biomechanics: mechanical properties of living tissues, 2nd ed. New York: Springer; 1993. p 568.

20. Billiar K, Sacks M. Biaxial mechanical properties of fresh and glutaraldehyde treated porcine aortic valve cusps: Part I. Experimental findings. J Biomech Eng. 2000;122:22–30.

21. Sacks MS. A method for planar biaxial testing that includes in-plane shear. J Biomech Eng 1999;121:551–555.

22. Fung Y. Foundations of solid mechanics. In: Fung Y, editor. Prentice-Hall international series in dynamics. Englewood Cliffs, NJ: Prentice Hall, 1965. p 525.

23. Press WH, Flannery BP, Teukolsky SA, Vetterling WT. Numerical recipes in C. Cambridge, UK: Cambridge University Press; 1988.

24. Kang T, Resar J, Humphrey JD. Heat-induced changes in the mechanical behavior of passive coronary arteries. J Biomech Eng 1995;117:86–93.

25. Rigby R, Hiraj N, Spikes J, Eyring H. The mechanical properties of rat tail tendon. J Gen Physiol 1959;43:265–282.

26. Billiar K, Sacks M. Biaxial mechanical properties of fresh and glutaraldehyde treated porcine aortic valve cusps: Part II. A structurally guided constitutive model. J Biomech Eng. To appear.

27. Lanir Y. A structural theory for the homogeneous biaxial stress–strain relationships in flat collageneous tissues. J Biomech 1979;12:423–436.

28. Sacks MS. A structural constitutive model for pericardium that utilizes SALS-derived fiber orientation information. J Biomech Eng. To appear.

29. Sacks M. A structural model for chemically treated soft tissues. In: Wayn JS, editor, ASME IMECE Vol. BED 43. Nashville, TN: ASME; 1999. p 101–102.

30. Sacks MS. A structural constitutive model for chemically treated planar connective tissues under biaxial loading. Comput Mech. To appear.

31. Billiar KL, Sacks MS. A method to quantify the fiber kinematics of planar tissues under biaxial stretch. J Biomech 1997;30:753–756

32. Billiar K, Sacks M, Singh G, Thompson K. Collagen fiber mobility under biaxial stretch. In: Fifth World Biomaterials Congress. Toronto: University of Toronto Press; 1996.

33. Orberg J, Baer E, Hiltner A. Organization of collagen fibers in the intestine. Connect Tissue Res 1983;11:285–297.

34. Orberg JW, Klein L, Hiltner A. Scanning electron microscopy of collagen fibers in intestine. Connect Tissue Res 1982;9:187–193.